

# A Study for Prevention of Unconfined Vapor Cloud Explosion from Spilled LNG Confined in Dike

Won K.Kim, PE, Professor at Fire Protection Engineering Lab of Seoul National University, Korea  
Hans-Christen Salvesen, Dr. Scient., GexCon, Norway

## Abstract

Spilled LNG (Liquefied Natural Gas) in a large scale can produce very cold vapor and the vapor will in general remain heavier than air until it absorbs heat from the surface of dike and surrounding air. If the cold vapor forms a fuel-air cloud heavier than air, then it may find an ignition source on the ground surface and cause an Unconfined Vapor Cloud Explosion (UVCE) during the process of dispersion. The object of this study is to investigate whether a flammable fuel-air cloud can be formed outside of the dike area in case of LNG spill made inside of the dike area. Evaporation and dispersion were modeled to predict the formation of a flammable vapor cloud. Some protection measures were also considered in the modeling to estimate the efficiency of those measures. Important input variables for dispersion modeling are size of LNG pool, wind direction and speed, insulation of dike floor, mitigation with high expansion foam, and vapor fence. The FLACS code, a computational fluid dynamics simulator, was used in dispersion modeling. The evaporation was modeled by analyzing heat transfer through conduction, convection and radiation. Results of the study show that a major leakage of LNG in the dike area could evaporate and flow over the dike wall and form a flammable cloud at the ground level outside the dike. This is different from what people have thought about natural gas. As NG is lighter than air at normal temperature, people have paid less attention to the UVCE risk of cold NG. Mitigation measures preventing from forming a large explosive cloud outside of the dike were also analyzed.

## 1. Introduction

Among the potential consequences from LNG leak accidents in LNG storage and processing facilities, Unconfined Vapor Cloud Explosion (UVCE) might be the worst one. But, the risk of UVCE from the spilled LNG has not been well introduced to the industries. Firstly most of them are not aware of the fact that density of methane (major hydrocarbons in natural gas) can be higher than air at cold temperatures. Most of industry people have experience with small size leak of LNG. In this case vapor can absorb heat from ground or surrounding air quickly and it becomes lighter than air. Once vapor becomes lighter than the air it moves up instead of spreading near the ground. Then, there is little chance for ignition. Industry people have been misled by the concept of vent stack of NG (gasified LNG). The system just discharges the NG to the air without burning it, because it is lighter than the air and could be discharged to the air safely. This is why people in the LNG facilities are not aware of UVCE risk. Some old facilities have UVCE protection system. But, due to the lack of perception of UVCE, the system is often not well maintained. And some of the new facilities do not consider the protection against UVCE at all. The purpose of this study is to address the potential hazard of UVCE from spilled LNG, and propose goals and requirements of existing protection systems. Evaporation from spilled LNG was modeled under different conditions. Dispersion of evaporated LNG was modeled by CFD code FLACS. Heat flux from LNG pool fire was calculated.

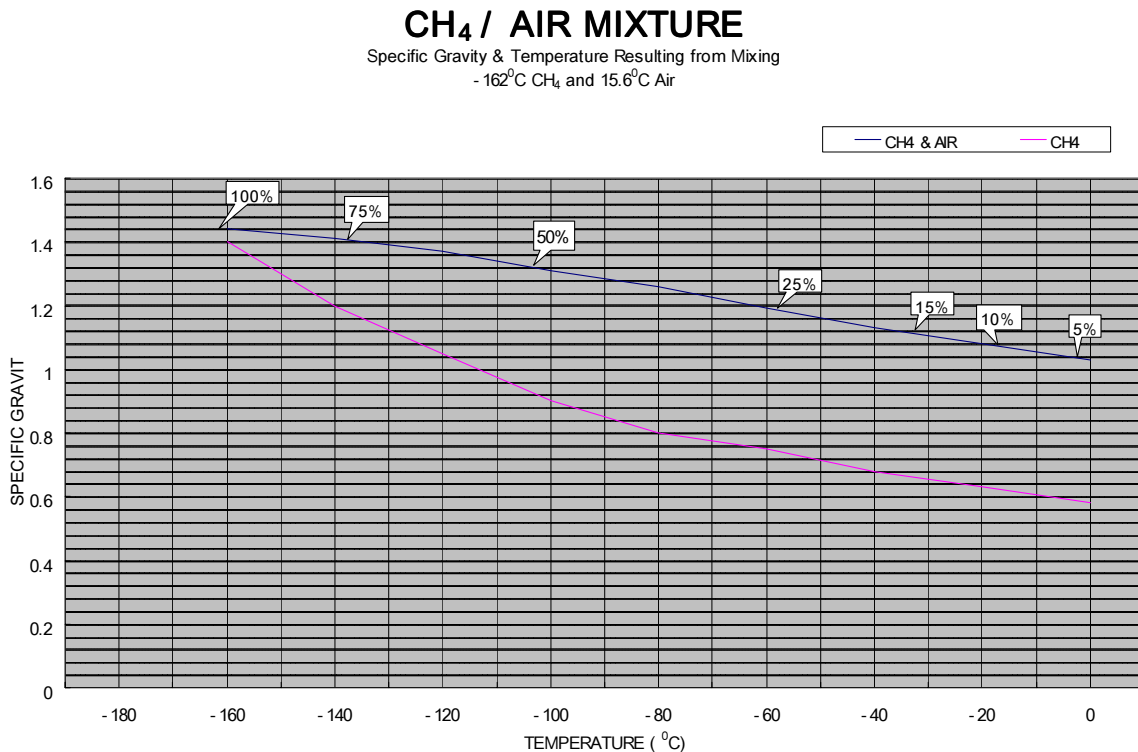
## 2. Methane/Air Density

### 2.1 Composition of LNG

Typical LNG consists of 85 to 95 % of methane, 7 to 10 % of ethane, 0 to 2 % of propane, 0 to 1 % of normal butane and 0 to 1 % of isobutene. Thus, methane is selected as a major component of LNG, in this study. The physical properties of methane are as follow;

□ Molecular Weight	16.0g/mol
□ Normal freezing Point	90.7K (-182.5°C)
□ Normal boiling Point	111.7K (-161.5°C)
□ Liquid Density	0.425g/cm <sup>3</sup> (at normal boiling point)

Mass density of vapor is a very important factor in assessing the possibility of ignition. The density of methane at atmospheric pressure divided by the density of air at the same temperature as methane is 0.55 (dividing molecular weight of methane 16g/mol by that for air 29.0g/mol and using the ideal gas law) However, cold vapor evaporated from LNG is heavier than air at normal temperature until it absorbs sufficient heat from entrained air and surroundings during dispersion. Thus, vapor from spilled LNG may spread near the ground in the beginning and it may find an ignition source away from the leakage area. In Fig. 1 the specific gravity is plotted versus temperature for pure methane and a mixture where 15.6°C air is added to -161.5°C methane. The specific gravity is defined as the mass density of the considered substance at normal pressure (1atm) and given temperature divided by the mass density of air at normal pressure and standard temperature 15.6°C.



Note : The percent values given in plots are volume percent

Figure 1. Specific gravity of pure Methane and of Methane/Air Mixture <sup>[1]</sup>

### 3. Model of Evaporation and Dispersion from Spilled LNG in Dike

A heat balance per unit area can be set up for the evaporating pool;

$$q_e = q_s + q_{con} + q_{rad} + q_{cool} \quad (1)$$

Where  $q_e$  [ $W/m^2$ ] is the evaporation heat flux,  $q_s$  [ $W/m^2$ ] represents the heat conduction from the subsoil,  $q_{con}$  [ $W/m^2$ ] is the convective heat transport from the air to the pool (due to wind),  $q_{rad}$  [ $W/m^2$ ] is the net in-radiated heat-flow, and  $q_{cool}$  [ $W/m^2$ ] represents the cooling down of the pool (this term can also represent heating depending on the sign of the term).

The evaporation heat flux is modeled by

$$q_e = m'' h_v, \quad (2)$$

where  $m''$  [ $kg/(m^2 \cdot s)$ ] is the evaporation flux and  $h_v$  [ $J/kg$ ] is the heat of vaporization.

The heat conduction from the subsoil is modeled by

$$q_s = \lambda_s(T_s - T_1)/\sqrt{(\pi a_s t^*)} \quad (3)$$

$$t^* = t - t_{start} \quad (4)$$

where  $\lambda_s$  [ $W/(m \cdot K)$ ] is the thermal conductivity (set to  $0.9 W/(m \cdot K)$  for average ground in all runs except mitigation runs 11041 and 100061 where it is set to  $0.09 W/(m \cdot K)$ ),  $T_s$  [ $K$ ] is the initial temperature of the subsoil (set to  $301.25^\circ K$  in the dispersion simulations),  $T_1$  [ $K$ ] is the temperature of the liquefied gas (initially equal the normal boiling point, the temperature will in general become lower after some time because of evaporation due to wind),  $a_s$  [ $m^2/s$ ] is the thermal diffusivity (set to  $4.3 \times 10^{-7} m^2/s$  for average ground in all runs), and  $t^*$  [ $s$ ] is the time after the evaporation has started at time  $t_{start}$  (in the dispersion simulations the evaporation starts at  $t_{start} = 10s$ ). The expression for  $q_s$  in Eq.3 can be rewritten;

$$q_s = F(t^*) \lambda_s (T_s - T_1) / \sqrt{(\pi a_s)} \quad (5)$$

$$F(t^*) = 1/\sqrt{(t^*)} \quad (6)$$

Since the time-factor  $F(t)$  in Eq.6 is singular with respect to time for  $t^* = 0s$ , a regular expression is used in the simulations when the time is small. The time-factor  $F(t^*)$  is redefined as

$$F(t^*) = 1.5 - 0.25t^*, \text{ when } 0 \leq t^* \leq 4 \\ 1/\sqrt{(t^*)}, \text{ when } 4 < t^* \quad (7)$$

Note that the time-factor  $F(t)$  redefined in Eq.7 is continuous as function of time for  $t^*=4s$ , and the integral with respect to time from  $t^*=0s$  to  $t^*=4s$  of the time-factor  $F(t^*)$  gives the same numerical value whether the function defined in Eq.6 or the one redefined in Eq.7 is used. The convective heat transport from the air to the pool is modeled by

$$q_{\text{con}} = \alpha_{\text{con}}(T_a - T_l) \quad (8)$$

$$\alpha_{\text{con}} d_{\text{pool}}/\lambda_a = 0.036\text{Re}^{0.8}\text{Pr}^{-0.33} \quad (9)$$

$$\text{Re} = \rho_a U_w d_{\text{pool}}/\mu_a \quad (10)$$

$$\text{Pr} = \nu_a/D_a \quad (11)$$

where  $\alpha_{\text{con}}$  [W/(m<sup>2</sup>·K)] is the heat transfer coefficient for convection,  $T_a$  [K] is the temperature of ambient air,  $T_l$  [K] is the temperature of the liquefied gas,  $d_{\text{pool}}$  [m] is the diameter of the pool (if the pool is not circular, the diameter of a circle with the same area as the pool is employed),  $\lambda_a$  [W/m K] is the thermal conductivity of ambient air,  $\text{Re}$  [-] is the Reynolds number,  $\text{Pr}$  [-] is the Prandtl number,  $\rho_a$  [kg/m<sup>3</sup>] is the density of ambient air,  $U_w$  [m/s] is the characteristic speed (in the code using local horizontal speed normalize to speed at height 10m above the pool corresponding to a logarithmic velocity profile with roughness length 0.005m),  $\mu_a$  [(N·s)/m<sup>2</sup>] is the dynamic viscosity of ambient air,  $\nu_a$  [m<sup>2</sup>/s] is the kinematic viscosity of ambient air, and  $D_a$  [m<sup>2</sup>/s] is the diffusion coefficient of ambient air. Note that the convective heat transport is not included in the model when the pool is boiling (after some time of the evaporation process, depending on the scenario, the pool will stop boiling).

Then net in-radiated heat-flow is modeled by

$$q_{\text{rad}} = (1 - \epsilon_z)q_z + \epsilon_a\sigma T_a^4 - \epsilon_p\sigma T_l^4 \quad (12)$$

where  $\epsilon_z$  [-] is the Albedo coefficient (set to 0.11),  $q_z$  [W/m<sup>2</sup>] is the solar radiation (set to 245.7W/m<sup>2</sup> in the simulations),  $\epsilon_a$  [-] is the emission coefficient for the radiation from the surroundings to the liquid pool (set to 0.95), and  $\sigma$  [W/(m<sup>2</sup>·K<sup>4</sup>)] is the Stefan Boltzmann constant.

The cooling down of the pool is modeled by

$$q_{\text{cool}} = -\delta_{vl}\rho_{vl}c_{vl}(dT/dt) \quad (13)$$

where  $\delta_{vl}$  [m] is the depth of the pool,  $\rho_{vl}$  [kg/m<sup>3</sup>] is the density of the liquefied gas, and  $c_{vl}$  [J/(kg·K)] is the specific heat of the liquid. In the numerical simulation the temperature of the pool is assumed to be uniform and a heat balance is calculated for the whole pool. The initial mass of the pool liquid is 700kg in the runs with a small pool filling the sump area, and 36.471x10<sup>6</sup>kg in the runs with a large pool filling the whole dike.

The evaporation flux is due to boiling (the temperature of the pool is not raised above the normal boiling point) and due to wind passing over the liquid surface. The evaporation due to wind  $m''_{\text{wind}}$  [kg/(m<sup>2</sup>·s)] is in general modeled by

$$m''_{\text{wind}} = 2 \times 10^{-3} U_w^{0.78} r_{\text{pool}}^{-0.11} M_{vl} \psi_p / RT_l \quad (14)$$

$$\psi_p = P_{\text{tot}} \ln(1 + P_w / (P_{\text{tot}} - P_w)) \quad (15)$$

where  $r_{\text{pool}}$  [m] is the radius of the pool,  $M_{vl}$  [kg/kmol] is the molecular weight of the liquid,  $P_{\text{tot}}$  [Pa] is the total pressure (atmospheric pressure set to 1.01325x10<sup>5</sup>Pa in the simulations),

and  $P_w$  [Pa] is the partial vapor pressure at the liquid level (this pressure will always be equal or less the total pressure). Since the factor  $\psi_p$  is singular in the limit when  $P_w$  approaches  $P_{tot}$  a modified expression is used in the model when  $P_w$  is close to  $P_{tot}$ :

$$\begin{aligned} \psi_p &= P_{tot} \ln(1 + P_w / (P_{tot} - P_w)), & \text{when } 0 \leq P_w \leq 0.95 P_{tot} \\ &= 3.1534 P_w, & \text{when } 0.95 P_{tot} < P_w \leq P_{tot} \end{aligned} \quad (16)$$

Note that  $\psi_p$  defined by Eq.16 is continuous as function of  $P_w$  (with  $P_{tot}$  fixed) for  $P_w = 0.95 P_{tot}$ .

The modeling of evaporation from a pool is based on theory found in the literature, cf. Refs.[5],[6],[7],[8].

The FLACS simulator was used to model dispersion from the spilled LNG in dike. FLACS is a complete dedicated 3-dimensional CFD simulation tool for ventilation, gas dispersion and explosions. It is developed, supported and maintained by GexCon AS, Bergen, Norway. FLACS has been validated against a large set of experimental data, including the recent full-scale experiments. The code is in general predicting within an accuracy of 30%. It uses a structured, fixed, rectangular grid. Additional blocks (multi-block concept) may be used for blast propagation. It uses a so-called backward Euler time integration scheme (1<sup>st</sup> order and 2<sup>nd</sup> order presently available). The spatial schemes are of type 2<sup>nd</sup> order upwind (Van Leer's scheme, Leonards Quick scheme). The SIMPLE algorithm of Patankar is used to solve the pressure-velocity coupling. The linear equations are solved by efficient solvers (BICGSTAB or TDMA).

#### 4. The implemented geometry of the tank and the dike, and the spill conditions

In the coordinate system used during the numerical calculations, the x-direction and the y-direction are in the horizontal plane, and the positive z-direction corresponds to vertically upwards. A tank is modeled with center in  $x = 200.0\text{m}$ ,  $y = 200.0\text{m}$ . The radius of the cylindrical tank is 30.68m, and in the vertical direction the tank extends from  $z = 0.0\text{m}$  (the ground level) to  $z = 56.0\text{m}$  (the top of the tank). Outside the tank the dike is modeled. The wall of the dike has inner radius 67.65m and outer radius 68.5m. In the vertical direction the wall extends from  $z = 0.0\text{m}$  (the ground level) to  $z = 8.4\text{m}$  (the top of the wall). Outside the dike area only flat ground at  $z = 0.0\text{m}$  is included in the geometrical model. This geometrical representation is used when a small pool in the sump area is modeled. It is assumed that the small pool fills up the sump area so that the upper surface of the pool is at the same level of the rest of the dike, i.e. at  $z = 0.0\text{m}$ . In some of the simulations a large pool of LNG fills up the whole dike so that the upper surface of the pool is at  $z = 7.37\text{m}$ . This upper surface is modeled in the geometrical model employed in these simulations. In two of dispersion simulations a higher wall surrounding the dike is implemented as a mitigation measure, the wall of the dike is increased from 8.4m to 18.4m. In one of these mitigation simulations a large pool of LNG fills up the whole dike so that the upper surface of the pool is at  $z = 7.37\text{m}$ . In another of these mitigation simulations a small pool fills up to the sump area so that the upper surface of the pool is at the same level as the rest of the dike, i.e. at  $z = 0.0\text{m}$ .

The grid resolution in the simulations is 3m in the horizontal plane in the central parts of the computational domain near the tank and the dike area, the grid is stretched towards the

boundaries of the computational domain. In the vertical direction the grid resolution in the simulations is approximately 1m from the ground level at  $z = 0.0\text{m}$  to a few meters above the top of the wall of the dike (8.4m high except in two mitigation simulations where it is 18.4m high), the grid is stretched towards the upper boundary of the computational domain. The computational domain extends in x-direction from  $x = -50\text{m}$  to  $x = 450\text{m}$ , in y-direction from  $y = 0\text{m}$  to  $y = 700\text{m}$ , and in z-direction from  $z = 0\text{m}$  to  $z = 200\text{m}$ .

Cross sectional view of tank and dike is shown in Figure 2.

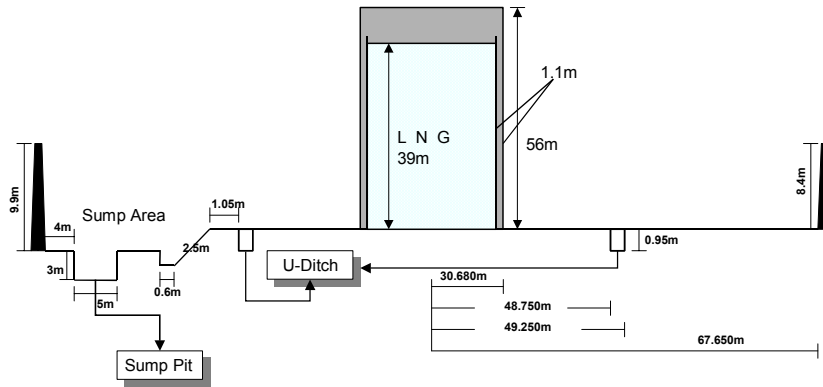


Figure 2, Cross sectional view of tank and dike

## 5. Computational results

The LNG pool is modeled as pure methane since in the present version of FLACS evaporation from a pool can only be modeled for a single component. To model LNG by pure methane is regarded to be a good approximation since the LNG contains 85–95% of methane. 13 dispersion simulations are performed for different scenarios. The pool is either a small pool filling the sump area or a large pool filling the whole dike. The wind speed of the external wind is 3.7m/s, 2.0m/s or 7.0m/s. This is the wind speed at the reference height 10.0m above the ground level, the vertical wind profile of the external wind is logarithmic with roughness length of the ground being 0.015m. The velocity vector of the external wind field is pointing in the positive y-direction.

A wind boundary condition is specified for the boundaries in the negative y-direction, the positive x-direction and the negative x-direction. An open boundary condition is specified in the positive y-direction. The so-called SYMMETRY boundary condition is applied at the boundaries in the positive z-direction and the negative z-direction (i.e. the ground), where there is no convection normal to the boundary. For the scenarios with a large pool filling the whole dike the problem is symmetrical in nature so only one wind direction is considered. For the scenarios with a small pool filling only the sump area, two wind directions are considered relative to the orientation of the pool. In the coordinate system the wind always comes from the negative y-direction, but the small pool area is specified for two different orientations.

Three mitigation measures are considered in the present study. One mitigation measure is to reduce the thermal conductivity for the subsoil from 0.9W/(m K) to 0.09W/(m K) (the effect of this is that the heat conducted from the subsoil to the pool is reduced to 10%). This reduced thermal conductivity for the subsoil corresponds to insulation of the ground of the dike. Another mitigation measure is to increase the height of the wall of the dike from 8.4m to 18.4m. And another mitigation measure is to model the effect of high expansion foam covering the upper surface of the pool. This foam is supposed to reduce the evaporation. This effect will be modeled by setting the evaporation due to wind to a reduced factor, 0.1, of the expression used when foam is not present. The same will be done with the convective heat transport (i.e. due to wind), it is set to a reduced factor, 0.1, of the expression used when foam is not present. Note that the value of 0.1 for the reduced factor is a chosen value expected to give some indication how the high expansion foam affects the formation of a flammable cloud.

The evaporation from the pool starts at  $t = 10.0s$  in the simulations, this gives the wind field some time to build up before the evaporation starts (at the inlet the external wind field is increased from zero to the specified value from  $t = 0.0s$  to  $t = 2.0s$ ). The scenarios of the 13 dispersion simulations are given in the Table 1.

Table 1, Scenarios of 3 dispersion simulations. The small pool filling the sump area can be oriented in 2 ways relative the external wind field. Orientation 1 indicates the wind direction is parallel to the arc of the sump and orientation 2 indicates the wind direction is 45 degree to the arc of the sump.

Run #	Pool Size	Pool Orientation	Mitigation Measures	Wind Speed [m/s]
100021	small	1		3.7
100022	small	2		3.7
100031	small	1		2.0
100032	small	2		2.0
100041	small	1	High expansion foam at top of pool	3.7
100051	small	1	Wall of dike increased by 10m	3.7
100061	small	1	Thermal conductivity reduced to 10%	3.7
110021	large			3.7
110031	large			2.0
110041	large		Thermal conductivity reduced to 10%	3.7
110051	large			7.0
110061	large		High expansion foam at top of pool	3.7
120001	large		Wall of dike increased by 10m	3.7

## 5.1 Pool Fire Modeling

Radiant heat flux was calculated by emissive power method. Large pool fire indicates a whole dike fire and small pool fire means partial dike (sloped area of the dike) fire. Radiant heat flux was calculated by the following equation;

$$q_r'' = E_p \cdot \phi \cdot \tau \quad (17)$$

where  $q_r''$  [kw/m<sup>2</sup>] is radiant heat flux received from pool fire and  $E_p$  [kw/m<sup>2</sup>] is the emissive power radiated from pool fire.  $\phi$  is the view factor changed by the flame height, distance and diameter of pool fire.  $\tau$  is a transmissivity varies by the distance and relative humidity.

Pool fire modeling works were performed based on the three different pool size ; large pool fire from whole dike surface, small pool fire from sump area surface, and sump pool fire from sump pit surface.

### ① Large Pool Fire

Radiant Heat (kw/m <sup>2</sup> )	Vulnerability	Impact Diameter (m)
10	Fatality	150
20	LNG pipe explosion	93
37.5	Mechanical failure	47

### ② Small Pool Fire

Radiant Heat (kw/ m <sup>2</sup> )	Vulnerability	Impact Diameter (m)
10	Fatality	53
20	LNG pipe explosion	34
37.5	Mechanical failure	19

### ③ Sump Pool Fire

Radiant Heat (kw/ m <sup>2</sup> )	Vulnerability	Impact Diameter (m)
10	Fatality	4
20	LNG pipe explosion	0
37.5	Mechanical failure	0

## 5.2 Evaporation Modeling Result

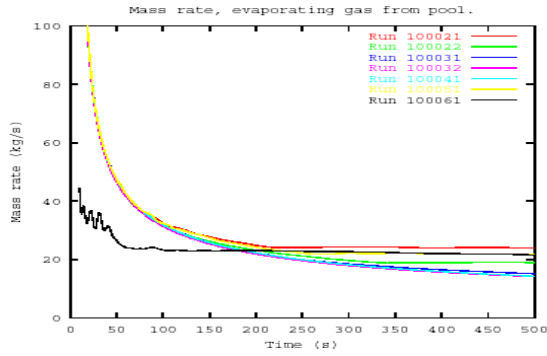


Fig.3, Mass rate of evaporating gas from pool, dispersion runs with the small pool filling the sump area

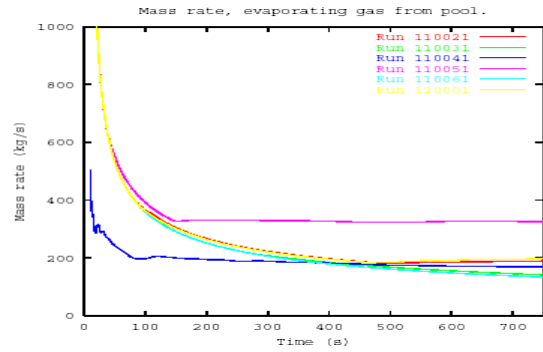


Fig.4, Mass rate of evaporating gas from pool, runs with the large pool filling the dike area

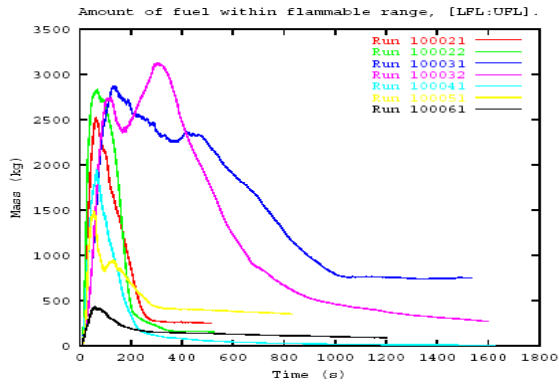


Fig.5, Amount of fuel [kg] within the flammable range plotted versus time. Runs with small pool filling the sump area

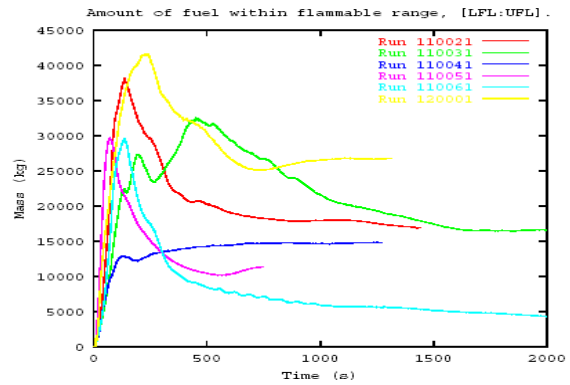


Fig.6, Amount of fuel [kg] within the flammable range plotted versus time. Runs with large pool filling the whole dike

## 5.3 Dispersion Modeling Result

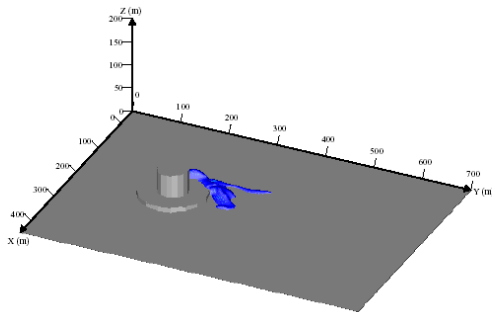
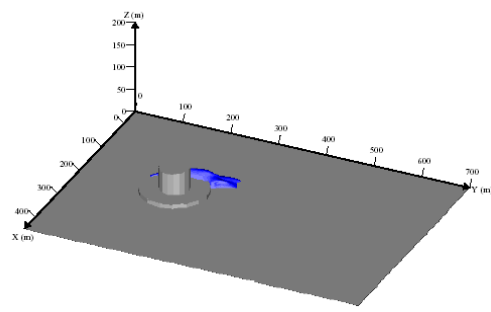


Fig.7, Run 100021, 3D volume plot of fuel-air cloud within flammable range at  $t = 70s$



Job:100022, Var:EELFL (-),  
Time:129.953 (s),I=1-98,J=1-102,K=1-30.

Fig.8, Run 100022, 3D volume plot of fuel-air cloud within flammable range at  $t = 130s$

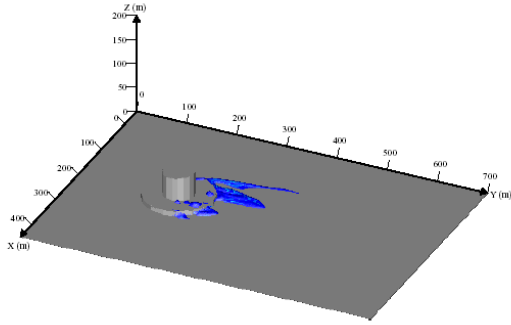


Fig.9, Run 100031, 3D volume plot of fuel-air cloud within flammable range at  $t = 140s$

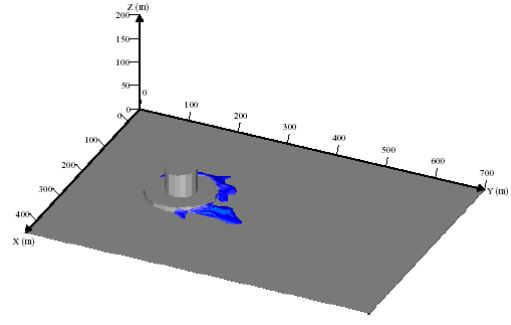


Fig.10, Run 100032, 3D volume plot of fuel-air cloud within flammable range at  $t = 300s$

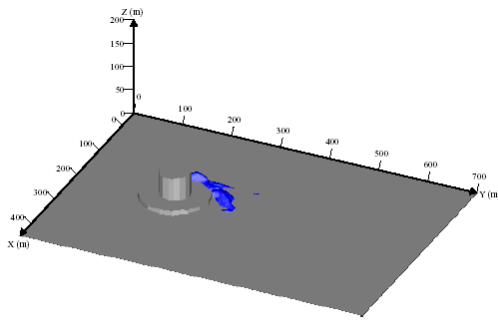


Fig.11, Run 100041, 3D volume plot of fuel-air cloud within flammable range at  $t = 70s$

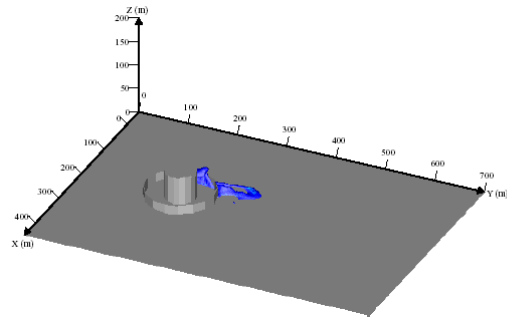


Fig.12, Run 100051, 3D volume plot of fuel-air cloud within flammable range at  $t = 60s$

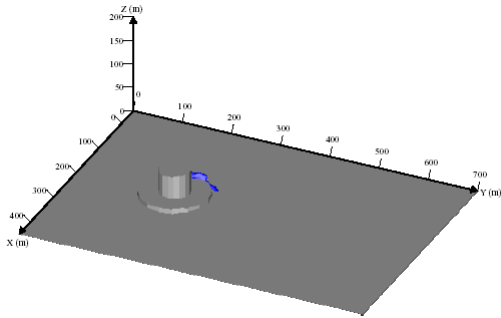


Fig.13, Run 100061, 3D volume plot of fuel-air cloud within flammable range at  $t = 60s$

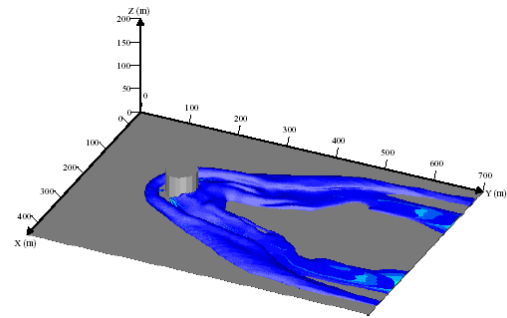


Fig.14, Run 110021, 3D volume plot of fuel-air cloud within flammable range at  $t = 160s$

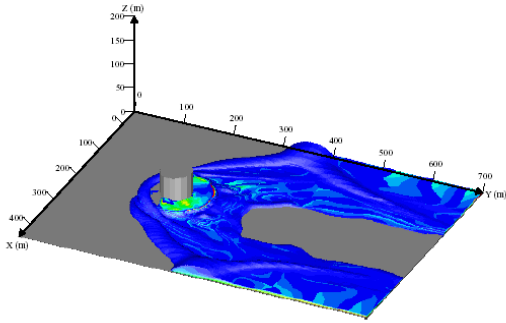


Fig.15, Run 110031, 3D volume plot of fuel-air cloud within flammable range at t = 500s

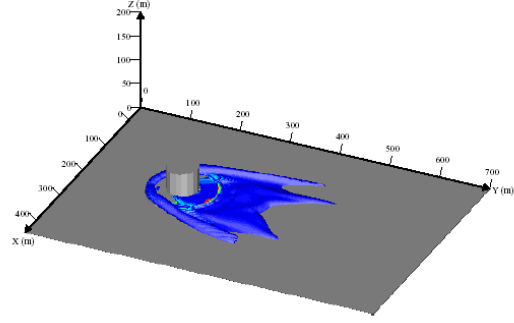


Fig.16, Run 110041, 3D volume plot of fuel-air cloud within flammable range at t = 800s

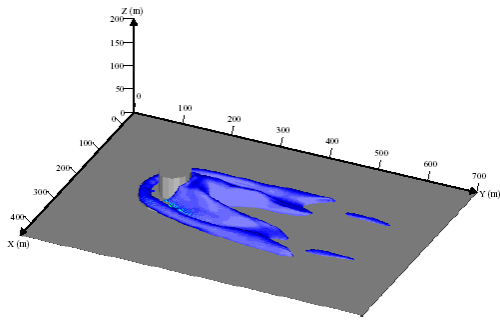


Fig.17, Run 110051, 3D volume plot of fuel-air cloud within flammable range at t = 80s

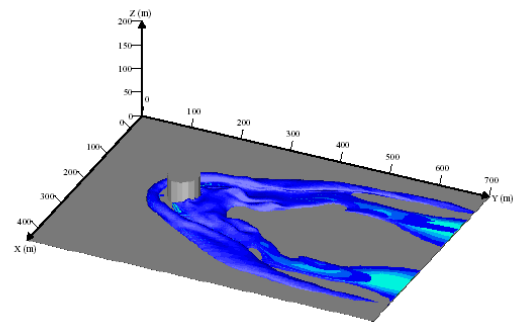


Fig.18, Run 110061, 3D volume plot of fuel-air cloud within flammable range at t = 140s

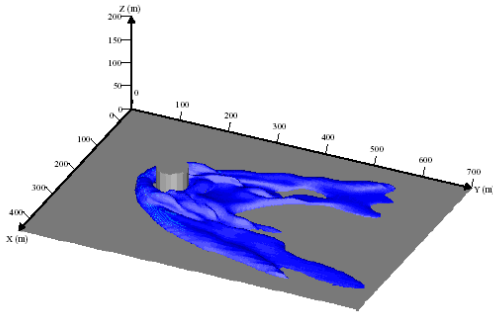


Fig.19, Run 120001, 3D volume plot of fuel-air cloud within flammable range at t = 250s

## 6. Analysis of Modeling Result

### 6.1 Radiant heat flux from pool fire

Exposure protection for pipes, valves, and cables are required in case of large and small pool fire. Fatalities can be caused from large and small pool fire.

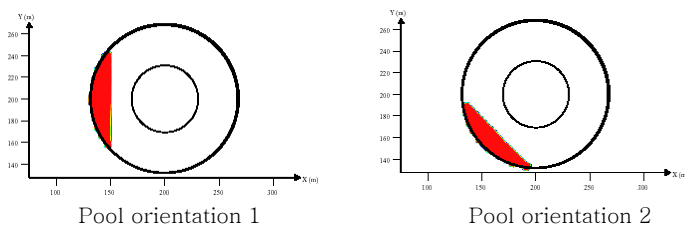
### 6.2 Evaporation

#### 6.2.1 Wind Speed

Varying the external wind speed for the small pool (other conditions fixed), the largest amount of fuel [kg] within the flammable range is for wind speed 2.0m/s compared to 3.7m/s. For the large pool, the largest amount of fuel [kg] within the flammable range is for wind speed 3.7m/s compared to 2.0m/s and 7.0m/s (other conditions fixed). This indicates that the effect of changing the external wind speed depends on the size of the pool.

#### 6.2.2 Wind Direction

Under the same external wind speed, but varying the pool orientation relative the external wind, the largest amount of fuel [kg] within the flammable range is for pool orientation 2.



Note ; Wind blows to + y direction.

### 6.3 Effect of Mitigation in Small Pool

With high expansion foam, the maximum (with respect to time) amount of fuel [kg] within the flammable range is reduced to 76.2% compared to case without this foam.

With height of dike wall increased by 10m, the maximum amount of fuel [kg] within the flammable range is reduced to 58.7% compared to case without this increase of wall height.

If the thermal conductivity of dike floor is decreased (representing insulation) to 0.1 of its original value, the maximum amount of fuel [kg] within the flammable range is reduced to 16.7% compared to the original condition.

In all these mitigation scenarios, the distance of dispersed fuel-air mixture within the flammable range was reduced.

#### 6.4 Effect of Mitigation in Large Pool

Covering LNG pool by high expansion foam reduced the maximum (with respect to time) amount of fuel [kg] within the flammable range to 77.6% of its original condition. Distance of dispersed flammable cloud was also reduced.

Vapor fence by 10m above the dike wall increased the maximum amount of fuel [kg] within the flammable range to 109.4% of its original condition. But, distance of dispersed flammable cloud was remarkably reduced.

Insulation at the dike floor (thermal conductivity decreased to 10%) reduced the maximum amount of fuel [kg] within the flammable range to 38.9% of its original condition. Here also, the distance of dispersed fuel-air mixture within the flammable range was reduced.

#### 7.0 Conclusion

It was found that vapor produced from large scale spillage of LNG can form explosive cloud over the dike wall and travel to process area. As there in general exist ignition sources outside of the dike area, the vapor dispersed outside of the dike wall can be ignited and explode. This may result in extensive property damage to the facility as well as fatalities. Thus, mitigation measures should be considered to protect against UVCE. And each mitigation design should be performed carefully. It is highly recommended to run a CFD code to model evaporation and dispersion when designing mitigation measures like those described in this paper.

## References

- [1] Thor Gjesdal, Hans-Christen Salvesen, Benoit Buffet, "FLACS Simulations of SMEDIS Scenarios", Technical Report, CMR-99-F30063, Christian Michelsen Research, Bergen, Norway, 1999, Confidential.
- [2] Hans-Christen Salvesen, Oddveig Asheim, "Simulation of Heavy Gas Dispersion with CFD code FLACS", Technical Report, CMR-95-F20021, Christian Michelsen Research, Bergen, Norway, 1995, Confidential.
- [3] Hans-Christen Salvesen, "Modeling of Jet Release of Liquefied Gas under High Pressure", Technical report, CMR-95-F20062, Christian Michelsen Research, Bergen, Norway, 1995, Confidential.
- [4] Torstein K. Fannelöp, "Fluid Mechanics for Industrial Safety and Environmental Protection", Industrial Safety Series, Volume 3, Elsevier Science, 1994.
- [5] "Methods for the Calculations of Physical Effects Resulting from Releases of Hazardous Materials", Bureau of Industrial Safety (TNO), CPR 14E, 1988.
- [6] "Methods for the Calculations of Physical Effects Resulting from Releases of Hazardous Materials", Bureau of Industrial Safety (TNO), CPR 14E, Third Edition, The Hague, 1997.
- [7] "Handbook for Fire Calculations and Fire Risk Assessment in the Process Industry", Scandpower A/S and Sintef – NBL, 2<sup>nd</sup> Edition, 1994.
- [8] Hans-Christen Salvesen, "NG dispersion modeling from spilled LNG confined in dike", Technical Report, CMR-00-F40018, GexCon, Bergen, Norway, January 2001, confidential.